IEEE Access
Multidisciplinary ⋮ Rapid Review ⋮ Open Access Journal

Received December 24, 2020, accepted January 6, 2021, date of publication January 11, 2021, date of current version January 21, 2021.

Digital Object Identifier 10.1109/ACCESS.2021.3050405

Single UWB Anchor Aided PDR Heading and Step Length Correcting Indoor Localization System

KELIU LONG[1,2], (Graduate Student Member, IEEE), CHONG SHEN[1,2], (Member, IEEE), CHUAN TIAN[4], KUN ZHANG[1,2,3], (Member, IEEE), UZAIR ASLAM BHATTI[5], DARRYL FRANCK NSALO KONG[1,2], SHUO FENG[1,2], AND HESEN CHENG[1,2]

[1]State Key Laboratory of Marine Resources Utilization in South China Sea, Hainan University, Haikou 570228, China
[2]College of Information Science and Technology, Hainan University, Haikou 570228, China
[3]Education Center of MTA, Hainan Tropical Ocean University, Sanya 572022, China
[4]Institute of Deep-sea Science and Engineering, Chinese Academy of Sciences, Sanya 572000, China
[5]School of Geography, Nanjing Normal University, Nanjing 210023, China

Corresponding authors: Chong Shen (chongshen@hainu.edu.cn), Chuan Tian (tianc@idsse.ac.cn), and Kun Zhang (kunzhang@hntou.edu.cn)

This work was supported in part by the National Key Research and Development Program of China under Grant 2017YFC0305903, in part by the High-level Talent Project of Hainan Natural Science Foundation under Grant 2019RC236, in part by the National Natural Science Foundation of China under Grant 61861015, and in part by the Key Project of Scientific Research of Higher Education in Hainan Province under Grant Hnky2019ZD-35.

ABSTRACT In this paper, we present a simple-structure Pedestrian Dead Reckon (PDR) system based on commercial IMU sensor and UWB ranging system. In PDR system, the accuracy of step and heading angle estimation completely decide the precision of location result. In order to select proper zero-velocity intervals for step and heading estimations in the foot stance/still stage, a modified zero-velocity detection way called Heuristic Step Detection (HSD) has been designed based on zero-velocity update algorithm (ZUPT). Based on the modified zero-velocity detection algorithm, i.e., HSD, an Kalman-type filter is used to get rough heading angle by fusing zero-velocity information and single UWB anchor ranging results. After that, a constrained sigma point based filter is used to further constrain heading angle range. Moreover, the range measures, provided by a UWB localization system with only one reference anchor, are used to correct the pedestrian step length. Trough UWB ranging measures analysis between two consecutive steps, the step length and pedestrian heading direction correcting processes are related to each other, and as a result, a more stable positioning result can be gotten. The corresponding practical experiments are conducted in real indoor environment over 2000 meters, and the results show that, compared with only INS-aided PDR, our scheme can reduce the average position error by more than 80%, and it can achieve long-term high accuracy and robust localization results.

INDEX TERMS Pedestrian dead reckon, ultra-wide band, indoor localization, fusion strategy.

I. INTRODUCTION

Nowadays, more and more intelligent services are based on real-time location, such as vehicle navigation [1], emergency service [2], and so on [3]. In outdoor scenarios, the Chinese BeiDou Navigation System (BDS), the Russian Gronus (GLONASS), the American Global Positioning System (GPS), and the European Galileo positioning and navigation system can provide comparatively high-quality location service [4]. However, due to the building and urban canyon blocking effect, the electromagnetic satellite signals will be attenuated or distorted under indoor environment [5]. Moreover, people spend most of time staying in room, it has great research potentiality and commercial value in indoor location system development. Therefore, many solutions have been designed to solve indoor localization problems. Inertia Navigation System (INS) is a self-constrained system, it can provide corresponding acceleration information and gyroscope readings of sensor motion in real time. In this reason, INS is being widely used in many indoor location scenarios. Pedestrian Dead Reckoning (PDR) is pedestrian localization approach aided by INS [6], [7], it can iteratively

The associate editor coordinating the review of this manuscript and approving it for publication was Kegen Yu.

and rapidly calculate the pedestrian position using heading information provided by INS and the given step length information. For example, A.R. Jiménez *et al.* implemented a Kalman-based framework to estimate walking people position and attitude [8]. In order to improve the properties of Micro-Electro-Mechanical System (MEMS) in pedestrian dead reckon, Hongyu Zhao *et al.* designed a two foot-mounted MEME localization system [9], which relies on symmetric drift and bias characteristics of IMU sensor to delimit the range of heading angle. Nevertheless, IMU has severe bias and drift on acceleration and gyroscope readings, and according to INS velocity and position solution rules, it only tracks short distance in acceptable accuracy [10], [11]. Although the former mentioned INS solutions can improve the tracking distance at some extend, these solutions have not been tested and verified in long-term localization experiment, especially in high motion state. Except for INS-based localization system, radio frequency-based localization systems have been exploited sufficiently in recent decades, such as ZigBee [12], [13] WIFI [14], [15] Ultra-Wideband (UWB) [16], [17] Bluetooth [18], [19] and so on. These radio frequency-based localization system mainly adopt Received Signal Strength Indication (RSSI) or ranging information to estimation target position [20]. More specifically, target position can be calculated according to RSSI distance formula or grid matching, its deployment and algorithm cost is extremely low. The drawbacks of RSSI way are low positioning precision and laborious signal strength map creating, and the positioning result is susceptible to environment [21]. Conversely, the ranging based positioning way can provide more accurate and stable results through calculating the distance between target and anchors while it costs much more than RSSI way. This method suffers from electromagnetic signal multipath effect and None-Line-of Sight (NLoS) [22]. Due to UWB system adopts nanosecond or sub-nanosecond pulse signal to ranging, UWB signal has strong anti-multipath ability and provides more stable positioning result. It is widely used in many kinds of localization scenarios, and the accuracy of UWB location system can reach centimeter level [23].

As is stated above, INS can provide continuous but inaccurate positioning result in long time scale. Conversely, UWB system can provide stable and discontinuous localization result. Therefore, many INS and UWB fusion localization algorithms have been proposed to further improve positioning accuracy. Yuan Xu *et al.* proposed a modified finite impulse response (UFIR) filter-based INS and UWB fusion system to improve indoor localization accuracy [24], and the Mahalanobis distance has been used to estimate the averaging horizon for the UFIR filter in real time. Jianan Zhu's team presented a hybrid filter, the Schmidt Kalman filter followed by a novel constrained sigma point based filter, for UWB-aided pedestrian location estimation under None Light of Sight (NLoS) and long-distance Light of Sight (LoS) situations [25]. After that, this team also proposed an adaptive localization based on the first-order Generalized Pseudo Bayesian (GPB) method to improve the localization accuracy under LoS and NLoS, which has achieved good localization accuracy [26]. Qigao Fan *et al.* designed a Double-State Adaptive Kalman Filter (DSAKF) algorithm based on Sage-Husa adaptive Kalman filter and fading adaptive Kalman filter to fuse INS and UWB localization results [27]. In order to extract useful information from UWB ranging results under NLoS environment, Beibei Li *et al.* used the maximum likelihood estimation algorithm to eliminate the influence of NLoS on the transmitted signal for better UWB system localization, and adopted the extended Kalman filter to fuse INS and UWB position result [5]. It could be seen that current indoor position researches are mostly concentrating on information fusion between INS and UWB localization system with multiple anchors. Although it can achieve a good localization result, the UWB system is a high cost set which limits its deployment area and universal application. In order to solve this problem, Qinglin Tian *et al.* proposed a Particle Filter (PF) based INS and UWB pedestrian localization fusion system with only one UWB anchor ranging measurements being used in this system [28]. This system fully uses the ranging measurements provided by UWB anchors to correct pedestrian positioning, and achieves good tracking results. However, this system has strict condition on phone placing attitude (keeping cellphone being in front of body and pointing to the direction of walking), and this system has not been tested under NLoS condition. And then, Qinglin Tian *et al.* designed a particle resetting approach to solve the lose tracking problem in PF based fusion system [3]. This approach has solved the lose tracking problem well in testing experiment. Same as former statement, this solution also adopts heading information provided by gyroscope embedded in cellphone, and only accelerometer data are used to detect step. Under the fact that mobile phone cannot be held parallel to ground strictly, it will incur great error in walking direction when it directly uses the yaw provided by IMU embedded in cellphone. Although the PDR assisted by one UWB anchor has achieved great progress in the localization accuracy, its potentiality has not been exploited sufficiently. In PDR, the step length and heading angle have severe impact on trajectory. The trajectory will gradually drift from real states when the step length or heading angle severely deviates from its true value.

Therefore, considering the localization system actual deployment cost and corresponding positioning accuracy, we propose a Direction and Step Correction Localization System (DSCLS) which is aided by one UWB anchor and an INS, its heading angle and step length can be constrained or estimated by UWB ranging data for better positioning accuracy. The main contributions of this paper are listed as follows:

1. Based on the traditional ZUPT, a step detection and zero-velocity selection algorithm, Heuristic Step Detection (HSD), is proposed in this paper. It can be used to detect step and sieve proper zero-velocity segment data for filter measurement updating. The HSD algorithm could improve the localization accuracy

properly when heading angle and step length are estimated at acceptable accuracy.

2. After that, heading angle dynamic restriction condition is set up and used to delimit pedestrian walking direction by using modified zero-velocity selection algorithm and transforming next step information into angle estimation form. It will reduce the distortion of whole trajectory.
3. And then, the step length estimation based on one UWB anchor ranging and heading information provided by previous process is discussed in our research, which improves the accuracy of pedestrian tracing distance and system stability.
4. At last, the several practical experiments, total testing distance over 2000 meters, are carried out to demonstrate our designs. The experiment results are compared and discussed under different conditions.

II. PROBLEM STATEMENT

The PDR is the most popular indoor pedestrian localization way, it uses the direction provided by IMU and estimated step length to iteratively compute the pedestrian location. Therefore, the heading angle, step length and step detection completely determine the localization result, the corresponding 2-Dimensional (2D) location updating equation is

$$\begin{bmatrix} x_k \\ y_k \end{bmatrix} = \begin{bmatrix} x_{k-1} \\ y_{k-1} \end{bmatrix} + \begin{bmatrix} \cos\theta \\ \sin\theta \end{bmatrix} * L_s, \tag{1}$$

where the x and y present coordinate values of selected navigation frame, k denotes the updating number or step number, and θ, L_s represents pedestrian heading angle and corresponding step length, respectively. As former statement, the initial location, heading angle and step length determine the localization accuracy.

In practical scenario, the initial location is prior knowledge, which could start from a known location such as building entrance and so on. The heading angle can be extracted from sensor fixed on pedestrian body or limbs. In some researches, the angle information is completely depending on the smartphone which being holding in hand and pointing to walking direction [28], [29]. However, the yaw information provided by cellphone is susceptible to hands shaking or cellphone attitude which is critical in initial alignment stage. Moreover, due to human non-rigid characteristic [9], hands holding smartphone way will influences the step detection and corresponding zero-velocity selection, and it has low practicability compared with IMU fixed on foot. The raw gyroscope readings using hands holding way and foot mounted way are shown in Fig. 1. As is depicted in Fig. 1(a), the hands holding way is hard to determine zero-velocity stage and step because of slight hands shaking and body swinging in walking state; conversely, as for foot-mounted way shown in Fig. 1(b), the IMU fixed on the foot has more stable characteristics in stance/still stage, it is easy to discern various walking states which benefit IMU measurement updating in filter and latter step length and heading angle correction.

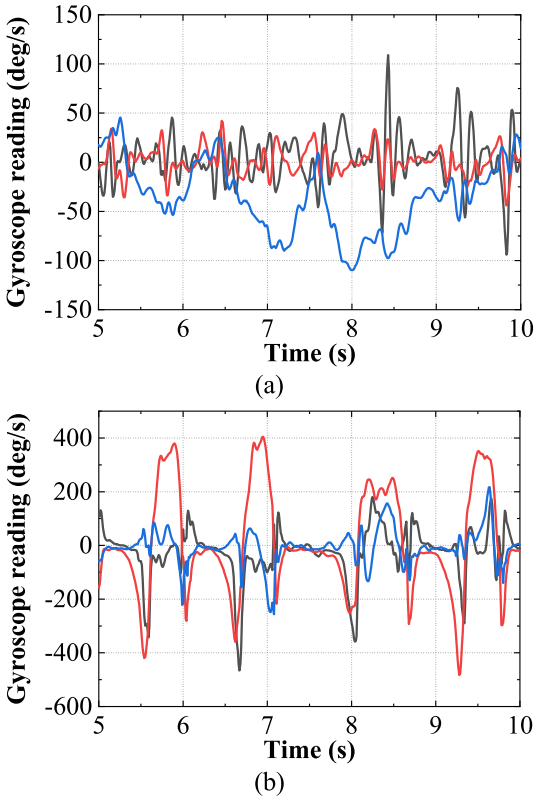

FIGURE 1. Comparison between hands holding IMU and foot fixing IMU in pedestrian walking state. (a) gyroscopic readings under hands holding way. (b) gyroscopic readings under foot-mounted way.

In PDR, the step length is commonly estimated by a model [28], formulated as

$$L_s = k_s{}^* h^* \sqrt{f_s}. \tag{2}$$

The coefficient, k_s, is a constant scaling factor which is different between male and female, h and f_s represent pedestrian height and walking frequency, respectively. This model can provide high accuracy of step length estimation. However, the distance error will be accumulated due to the minor step estimation error, and it may not exactly suitable for everyone. Therefore, the step length estimated by (2) should be corrected before being used to calculate location.

The pure INS localization system has been investigated sufficiently in the past decades; many solutions have been exploited to improve the reliability of localization results. Among them, the magnetometer and barometer embedded in MEMS are mostly used to correct motion direction and height [30], it has achieved better localization results compared with pure INS way. However, the magnetometer is susceptible to modern indoor harsh magnet environment, and the barometer readings are hard to be distinguished between two position with marginal height difference. Moreover, the commercial low-price MEMS sensors have significant bias and drift [8]. Hence, most researchers concentrate on correcting pedestrian location by fusing MEMS and UWB system localization results directly [5], [26], [27], [31], which need high density UWB anchor deployment accompanied with high costs.

It is the tradeoff between set costs and localization accuracy. Moreover, the position accuracy does not linearly increase with the number of UWB base stations when the base station number has reached a certain number. Therefore, the number of base stations should be reduced while keeping high localization accuracy.

III. PROPOSED PDR AND UWB FUSION SYSTEM

A. OVERVIEW

The data flow processing procedures of the proposed positioning system is shown in Fig. 2. This system is started with IMU raw data and sampling interval acquiring, and then step is detected by ZUPT. Since step frequency is lower than IMU sampling frequency and UWB updating frequency, the later processing progress is based on step detection, and the whole processing structure is triggered by new IMU data. After the step has been detected, in the ***Zero-velocity Interval selection*** block, the angular velocity and acceleration are adopted to choose a proper zero-velocity interval for IMU states updating. Due to ranging frequency of UWB system differing with frequency of pedestrian step and the UWB system may being in NLoS state, the UWB ranging measures should be sieved before being used for position estimation. ***In the UWB ranging R_k selection*** block, the time stamp of the selected UWB measure should be close to that of current detected step under LoS condition. The ***INS Update and error compensation*** strategy is implemented with Kalman-type Filter (KF). After that, by comparing current UWB ranging measurement with former step UWB ranging result, the ***Heading angle optimization*** or ***Step length optimization*** is executed respectively. At last, the optimal position is updated using former estimated results, and processing flow return to next circle. In later statement, the whole processing technology will be described in detail. It should be emphasized that the location of UWB anchor can be calculated by INS data in initial localization stage, which is proposed in [28]. However, the IMU used in this paper is commercial level, it suffers high drift and large bias and it will degrade its estimation accuracy severely. Therefore, the location of UWB anchor will be manually calibrated for better positioning result.

B. STEP DETECTION AND ZERO-VELOCITY INTERVAL SELECTION

In this paper, the ZUPT is chosen to implement initial step detection, it can judge the step characteristics by using angular velocity and acceleration provided by IMU. The detail of ZUPT is given in [8], and we simply describe it as follow three constraint conditions ($C1$, $C2$, $C3$):

$$C1 = \begin{cases} 1 & th_{a\min} < |a_k| < th_{a\max} \\ 0 & otherwise, \end{cases} \tag{3}$$

$$C2 = \begin{cases} 1 & \sigma_a > th_{\sigma_a} \\ 0 & otherwise, \end{cases} \tag{4}$$

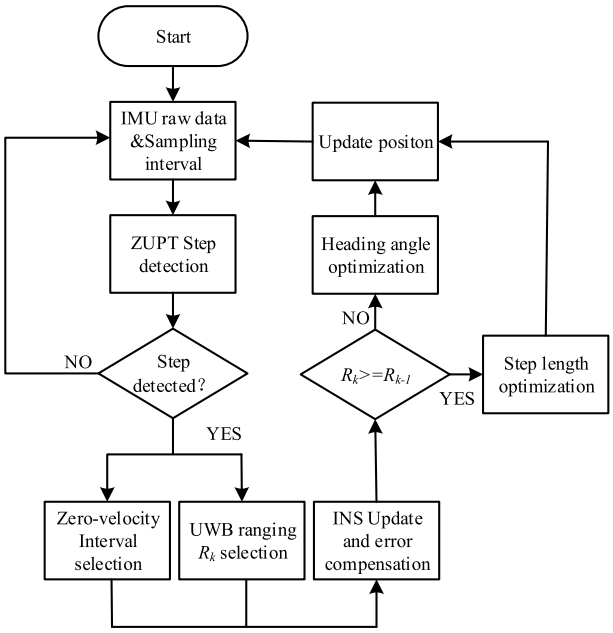

FIGURE 2. Structure of the proposed system for localization. R_k denotes the k-th UWB ranging measurement.

$$C3 = \begin{cases} 1 & |\omega_k| < th_\omega \\ 0 & otherwise, \end{cases} \tag{5}$$

$th_{a\min}$ and $th_{a\max}$ represent the 2-norm of k-th sampling acceleration $|a_k|$, lower bound and upper bound, respectively. σ_a is the root mean variance of acceleration under a selected window, and $th_{\sigma a}$ is corresponding threshold. $|\omega_k|$ denotes the 2-norm of k-th sampling angular velocity ω_k, and th_ω is the selected threshold.

As is stated above, there are five basic parameters (th_{amin}, th_{amax}, $th_{\sigma a}$, th_ω, and the window size), which should be determined before step-stance/still detection, and the values of these parameters should be different according to different people and motion type. Fig. 3 depicts different parameter values of ZUPT used in step detection and zero-velocity point selection, which is hard to select zero-velocity stage exactly and detect step correctly. In traditional way, the zero-velocity data are used to calibrate position and velocity. As is shown in Fig. 3, in ZUPT selected zero-velocity points, the corresponding angular velocity and acceleration is not absolute zero state or stay in stable interval, there are some fluctuations around ZUPT selected points. It may result in wrong step detection and invalid zero-velocity updating in IMU state estimation. Therefore, based on the ZUPT, we designed a zero-velocity selection way called Heuristic Step Detection (HSD) algorithm to acquire more reliable data for state calibration. The corresponding zero-velocity selection equation is as follow:

$$T1 = |d_k - ((d_k - |d_{k+t} - d_{k+2t}|) + (d_k - |d_{k+t} - d_{k+3t}|))/2|, \tag{6}$$

where d_k is k-th sampling data (acceleration or angular velocity), t denotes data selection window. If $T1$ is lower than

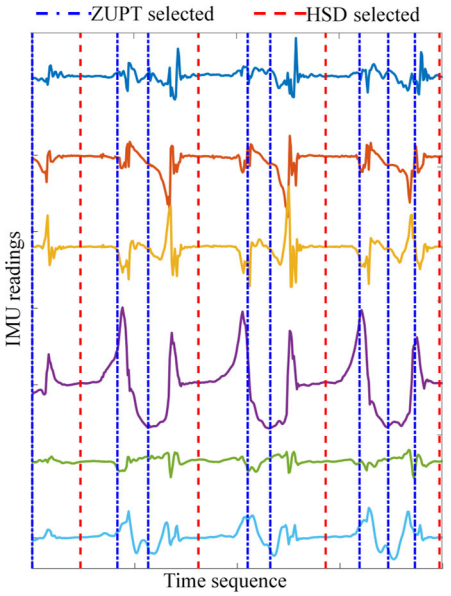

FIGURE 3. The zero-velocity interval midpoint selection using ZUPT and HSD respectively.

a given threshold th_{T1}, $T1 < \text{th}_{T1}$, the corresponding k-th sampling data can be used for state updating. In common case, the smaller th_{T1} is, the more precise result will be given. In order to acquire appropriate quality and quantity data, the threshold th_{T1} should be set properly.

C. INS UPDATE AND ERROR COMPENSATION

In INS localization system, the navigation frame (n-frame) is East-North-Up (ENU), the body frame (b-frame) is Right-Forward-Up (x_b-y_b-z_b), and the localization results are displayed in Cartesian coordinates as presented in Fig. 4. The IMU sensor and UWB tag are mounted on the foot, and IMU and UWB tag are tightly fixed which can be treated as a device in their geometric center.

In commercial application, the low-cost IMU cannot measure some physical effects which may increase computational complexity and reduce the accuracy of results, thus, it needs to ignore some physical effects in actual INS state calculation, such as the Earth's curvature and rotation, the centrifugal force, and the Coriolis force [9]. Therefore, the simplified INS state equation is given as

$$\begin{aligned} \dot{\boldsymbol{C}}_b^n &= \boldsymbol{C}_b^n \Omega_{ib}^b \\ \dot{\boldsymbol{v}}^n &= \boldsymbol{C}_b^n \boldsymbol{f}^b + \boldsymbol{g}^n \\ \dot{\boldsymbol{p}}^n &= \boldsymbol{v}^n, \end{aligned} \tag{7}$$

where the letters n, b and i denote the n-frame, b-frame and inertial coordinate frame for short, respectively; $\boldsymbol{C}_b^n$ is the direction rotation matrix; Ω_{ib}^b is the skew-symmetric matrix of gyroscope angular rate; $\boldsymbol{v}^n$ is the velocity in n-frame; the specific force is $\boldsymbol{f}^b$, and the gravity is $\boldsymbol{g}^n$. The direction rotation matrix can be converted form Euler angle $\boldsymbol{\varphi}$, the state vector of INS can be defined as $\boldsymbol{x}_k = [\boldsymbol{\varphi}_k^n, \boldsymbol{v}_k^n, \boldsymbol{p}_k^n]^T \in \mathbb{R}^9$.

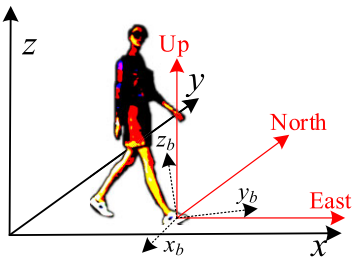

FIGURE 4. The sensor mounted on the foot.

After that, in order to provide more accuracy direction angle and better positioning result, the INS state equation should be corrected by two measures (zero-velocity update and UWB distance measure) as follows:

$$\begin{aligned} \delta\dot{\boldsymbol{\varphi}} &= -\boldsymbol{C}_b^n \delta\boldsymbol{\omega}_{ib}^b \\ \delta\dot{\boldsymbol{v}}^n &= (\boldsymbol{C}_b^n \boldsymbol{f}^b) \times \delta\boldsymbol{\varphi} + \boldsymbol{C}_b^n \delta\boldsymbol{f}^b \\ \delta\dot{\boldsymbol{p}}^n &= \delta\boldsymbol{v}^n, \end{aligned} \tag{8}$$

where $\delta\boldsymbol{\varphi}$ denotes the attitude error, $\delta\boldsymbol{v}$ is the velocity error, $\delta\boldsymbol{p}$ denotes the error vector of position. $\delta\boldsymbol{f}^b$ and $\delta\boldsymbol{\omega}_{ib}^b$ are measurement errors of acceleration and angular velocity, respectively. The error vector is defined as $\delta\boldsymbol{x}_k = [\delta\boldsymbol{\varphi}_k, \delta\boldsymbol{v}_k^n, \delta\boldsymbol{p}_k^n]^T \in \mathbb{R}^9$, and the corresponding KF state model is

$$\begin{aligned} \delta\boldsymbol{x}_k &= \boldsymbol{F}_k \cdot \delta\boldsymbol{x}_{k-1} + \boldsymbol{w}_{k-1} \\ \boldsymbol{y}_{vp,k} &= \boldsymbol{h}(\delta\boldsymbol{x}_k) + \boldsymbol{\eta}_{vp,k}, \end{aligned} \tag{9}$$

where

$$\boldsymbol{y}_{vp,k} = [\boldsymbol{v}_{ZUPT}, (\boldsymbol{d}_{k/k-1}^I)^2 - (\boldsymbol{d}_{k/k-1}^U)^2]^T, \tag{10}$$

$$h(\delta\boldsymbol{x}_k) = [\delta\boldsymbol{v}_k^n, (2(\boldsymbol{p}_{k/k-1}^I - \boldsymbol{p}^A) - \delta\boldsymbol{p}_k^n)(\delta\boldsymbol{p}_k^n)^T]_{1\times 4}, \tag{11}$$

$\boldsymbol{v}_{ZUPT}$ is actual velocity in selected zero-velocity interval, $\boldsymbol{d}_{k/k-1}^I$ and $\boldsymbol{d}_{k/k-1}^U$ are the distances between pedestrian foot and UWB anchor which are derived by INS and UWB system, respectively. $\boldsymbol{w}_{k-1}$ and $\boldsymbol{\eta}_{vp,k}$ are the independent Gaussian white noises. $\boldsymbol{p}_{k/k-1}$ denotes the IMU sensor position that has not been compensated by filter estimation in time instant k. $\boldsymbol{p}^A$ is the constant coordinate of UWB anchor.

$$\boldsymbol{F}_k = \begin{bmatrix} \boldsymbol{I}_{3\times3} & \boldsymbol{O}_{3\times3} & \boldsymbol{O}_{3\times3} \\ \boldsymbol{S}_k \cdot \Delta t & \boldsymbol{I}_{3\times3} & \boldsymbol{O}_{3\times3} \\ \boldsymbol{O}_{3\times3} & \boldsymbol{I}_{3\times3} \cdot \Delta t & \boldsymbol{I}_{3\times3} \end{bmatrix}, \tag{12}$$

$$\boldsymbol{H}_{vp} = \partial \frac{h(\delta\boldsymbol{x}_k)}{\delta\boldsymbol{x}_k}, \tag{13}$$

where $\boldsymbol{I}_{3\times3}$ is a 3×3 identity matrix, $\boldsymbol{O}_{3\times3}$ denotes the 3×3 zero matrix, Δt is the sampling interval, $\boldsymbol{S}_k$ denotes the skew-symmetric matrix of the specific force $\boldsymbol{C}_b^n \boldsymbol{f}^b$. And then, the Kalman filtering process can be used to provide the rough heading angle (extracting from Euler angle), and the heading angle can be constrained at some extent using UWB ranging in next stage.

D. UWB RANGING SELECTION

The accuracy of UWB ranging has effects on subsequent position estimation, it is affected by UWB NLoS signal judgement and step stance/still time detection. There are several ways to judge NLoS signal including neural network [32], the power-based way [33] and so on. In this paper, the power-based scheme is selected to find appropriate UWB ranging measurements under NLoS routines. In this way, the First Path Component (FPC) of UWB signal in receiver is the key to determine the signal reaching time and style (NLoS or LoS). More specifically, as is presented in (14), the power difference, Q_D, between the power of FPC, Q_{FPC}, and the total received power, Q_T, can be applied to judge whether UWB signal transmission is in LoS or NLoS. The UWB development kit used in our program is from DecaWave, which can provide Q_D by reading its register values C, $F1$, $F2$, and $F3$ and calculating according to (15). An empirical judgement standard can be given that the UWB transmission path is in NLoS when Q_D is greater than 10 dBm and in LoS when Q_D is less than 6 dBm [33]. All the variables used this subsection is in unit of dBm.

$$Q_D = Q_T - Q_{FPC}, \tag{14}$$

$$Q = 10log\left(C^*2^{17}/F_1^2 + F_2^2 + F_3^2\right). \tag{15}$$

In LoS condition (Q_D < 6dBm), the UWB ranging with timestamp closest to that of detected step is chosen to estimate pedestrian position. And in order to ensure the accuracy of localization system, the UWB ranging will be discarded when it is hard to discern (6dBm <= Q_D < 10dBm)) or stays in NLoS environment (Q_D >= 10dBm).

E. THE HEADING ANGLE AND STEP LENGTH OPTIMIZATION

In common scene, walking direction and step length are considered two separated variables. Meanwhile, pedestrian activity is a regular and reciprocating motion in a limited area, thus the distance between target and UWB anchor varies with time. In this section, walking direction is associated with step length for more stable position estimation. According to pedestrian motion characteristics and UWB ranging results, its motion state can be divided into three patterns by comparing current distance d_k between pedestrian and UWB anchor with former d_{k-1}: Pattern_1, approaching UWB base ($d_k < d_{k-1}$); Pattern_2, leaving UWB base ($d_k > d_{k-1}$); Pattern_3, keeping same distance with UWB base ($d_k = d_{k-1}$).

1) HEADING ANGLE OPTIMIZATION

The Pattern_1 of localization system is shown in two-dimension (2D) plane as presented in Fig. 5, where $R0$ and $R1$ are the distances from UWB anchor (X_A, Y_A) to Step_0 (X_0, Y_0) and Step_1 (the intersections of the red arrow and the circle shown in Fig. 5), respectively. It could be seen that the step length $L0$ between Step_0 and Step_1 cannot be directly determined with 2 intersections between the red arrow and the circle. However, we can give the heading angle range for

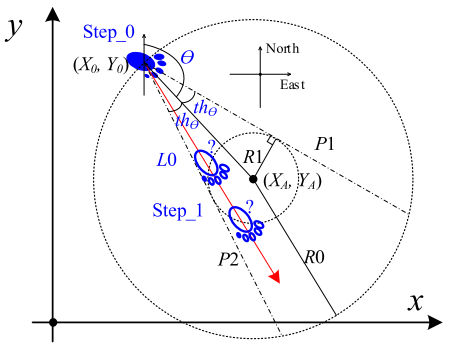

FIGURE 5. Pedestrian approaching the UWB base station. *P1* and *P2* are tangent of circle with radius *R0*.

improving direction accuracy according to R *(R0-R5)*. The radius R can be calculated by UWB anchor height (h) and corresponding measuring distance (M) at each step, i.e.,

$$R = \sqrt{M^2 - h^2}, \tag{16}$$

thus, the radius R can be considered as a constant in all calculations. Moreover, the locations of Step_0 (X_0, Y_0) and UWB base station (X_A, Y_A) have been known. More specifically, the location of Step_0 is initial position or former calculated position, and the position of UWB base station is a prior knowledge.

Therefore, as shown in Fig. 5, the range of pedestrian heading angle θ_H (the direction of red arow in Fig. 5) is

$$\theta - th_\theta <= \theta_H <= \theta + th_\theta, \tag{17}$$

where th_θ is half changing range of heading angle, and th_θ is

$$th_\theta = \arcsin(R1/\sqrt{(X_0 - X_A)^2 + (Y_0 - Y_A)^2}), \tag{18}$$

θ_H denotes heading angle, and θ ($-\pi < \theta \leq \pi$) is the angle between north direction and the line which links Step_0 position (X_0, Y_0) and anchor position (X_A, Y_A):

$$\theta = \begin{cases} \arctan(\dfrac{X_A - X_0}{Y_A - Y_0}), & Y_A - Y_0 > 0 \\ sign(X_A - X_0)\cdot\pi + \arctan(\dfrac{X_A - X_0}{Y_A - Y_0}), & Y_A - Y_0 < 0 \\ \dfrac{\pi}{2}, Y_A - Y_0 = 0, & X_A - X_0 > 0 \\ -\dfrac{\pi}{2}, Y_A - Y_0 = 0, & X_A - X_0 < 0. \end{cases} \tag{19}$$

According to the relation (17), it can be used to constrain the heading angle and provide better localization result. A constrained sigma-point based filter [25], [26] is selected as the optimal estimation process, it is divided into three stages:

Stage_1, given the $2n + 1$ sigma points $\hat{\boldsymbol{\chi}}$ as

$$\hat{\boldsymbol{\chi}}_i = \begin{cases} \boldsymbol{x}_s, & i = 0, \\ \boldsymbol{x}_s + [\sqrt{(n+k)\boldsymbol{P}_s}]_i, & i = 1:n, \\ \boldsymbol{x}_s - [\sqrt{(n+k)\boldsymbol{P}_s}]_{i-n}, & i = n+1:2n, \end{cases} \tag{20}$$

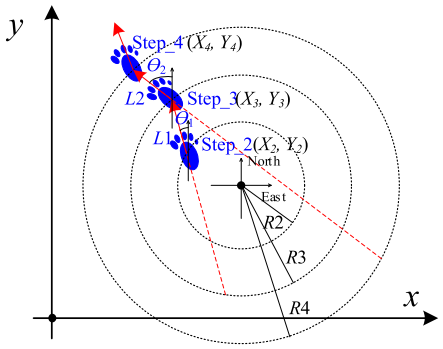

FIGURE 6. The pattern_2 of localization system. *L2* and *L1* are step length, and $\emptyset_1$ and $\emptyset_2$ denotes pedestrian walking direction.

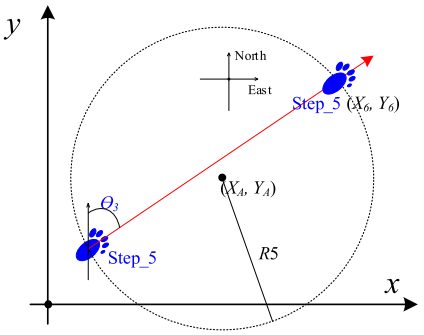

FIGURE 7. The diagram of Pattern_3.

where $k \in \mathbb{R}$ is used for turning the size of sigma point distribution. $\boldsymbol{x}_s$ denotes the former mentioned state vector of INS $\boldsymbol{x}_s = [\boldsymbol{\varphi}_s^n, \boldsymbol{v}_s^n, \boldsymbol{p}_s^n]^T \in \mathbb{R}^9$, $\boldsymbol{P}_s$ is selected as the covariance matrix of former Kalman filtering stage in *Section C*. n denotes the dimension of estimation state, and $[\sqrt{(n+k)\boldsymbol{P}_s}]_i$ presents the i-th column of the matrix $\sqrt{(n+k)\boldsymbol{P}_s}$.

Stage_2, all the sigma points are calculated through following correction update:

$$\hat{\boldsymbol{\chi}}_i^+ = \arg\min(\boldsymbol{x} - \hat{\boldsymbol{\chi}}_i)^{\mathrm{T}} \boldsymbol{W} (\boldsymbol{x} - \hat{\boldsymbol{\chi}}_i), \quad \text{subject to } \theta - th_\theta <= \theta_H <= \theta + th_\theta, \tag{21}$$

where $\boldsymbol{W}$ is the weight matrix which is set as covariance matrix $\boldsymbol{P}_s$, $\theta_H$is the yaw component of state x which could be gotten from (7).

Stage_3, calculating the corrected estimation and its corresponding covariance:

$$\hat{\boldsymbol{x}}_2^+ = \sum_{i=0}^{2n} \omega_i \hat{\boldsymbol{\chi}}_i^+, \tag{22}$$

$$\boldsymbol{P}_2^+ = \sum_{i=0}^{2n} \omega_i (\boldsymbol{\chi}_i^+ - \hat{\boldsymbol{x}}_2^+)(\boldsymbol{\chi}_i^+ - \hat{\boldsymbol{x}}_2^+)^{\mathrm{T}}, \tag{23}$$

where $\omega_i = \begin{cases} k/(n+k), & i = 0 \\ 1/(2(n+k)), & i = 1, 2, ...n. \end{cases}$

The estimation result, $(\hat{\boldsymbol{x}}_2^+, \boldsymbol{P}_2^+)$, is the output of the block ***Heading angle optimization*** in Fig. 2. The result $\hat{\boldsymbol{x}}_2^+$contains optimized heading angle. $\boldsymbol{P}_2^+$can be used as covariance matrix in next Kalman filtering stage.

2) STEP LENGTH OPTIMIZATION

The Pattern_2 of the proposed system is pedestrian departing from UWB anchor as shown in Fig. 6. In this pattern, the heading angle cannot be constrained by the condition provided by Pattern_1, it completely depends on former fusion estimation (***INS Update and error compensation*** block in Fig. 2), and the fusion estimation can adopt traditional fusion way, i.e., magnetometer [34] multi-INS fusion [35] and so on, to correct the pedestrian direction. In Pattern_2, taking the walking direction into consideration, the step length can be calculated through the UWB ranging and heading angle. It can assume that the coordination of Step_2 (X_2, Y_2) has been obtained in former estimation process or initial prior knowledge (starting from a known point), the coordination of Step_3 (X_3, Y_3) shown in Fig. 6 can be gotten by following solving equations:

$$\begin{cases} \cot(\theta_1)(X - X_2) = (Y - Y_2) \\ X^2 + Y^2 = R_3^2. \end{cases} \tag{24}$$

It is obvious that (24) has two solutions, and step lines (red dash line) shown in Fig. 6 has two intersections with a ranging circle. However, the step line is a vector (a line with walking direction) which can provide the only intersection ($X3$, $Y3$) with ranging circle. After that, the step length $L1$ can be given as

$$L1 = \sqrt{(X_3 - X_2)^2 + (Y_3 - Y_2)^2}. \tag{25}$$

The Pattern_3 shown in Fig. 7 is the special case of Pattern_1 and Pattern_2, which can calculate the step length by using (24) in Pattern_2. Moreover, it can also can provide the walking direction by giving the step length estimated in former stage. Specifically, heading angle and step length can be simultaneously estimated in Pattern_3.

3) UPDATING POSITION

After the whole optimal procedure being done, the pedestrian location is updated with former optimal estimation result including heading direction and step length.

IV. EXPERIMENTAL SETUP AND VERIFICATION

The IMU sensor are synchronized with the UWB system in host computer, and the timestamp of PDR is set as corresponding IMU sensor timestamp when a valid step is detected. Since the UWB localization system is MDEK1001 Development Kit from DecaWave, and its updating frequency is up to 10Hz. In normal indoor scenario, the frequency of pedestrian step is lower than that of UWB system. Therefore, the valid UWB measurement (under LoS scenario) with closest timestamp to PDR measurement should be selected for location calculation when a step is detected. The IMU sensor relative parameter is listed in Table 1.

The layout of the experiment area is shown in Fig. 8, it is a 29.74m × 9.39m office and laboratory hybrid area with a corridor. The 2-Dimensional (2D) Cartesian coordinate is established with unit of meter, and the point S4 is defined as

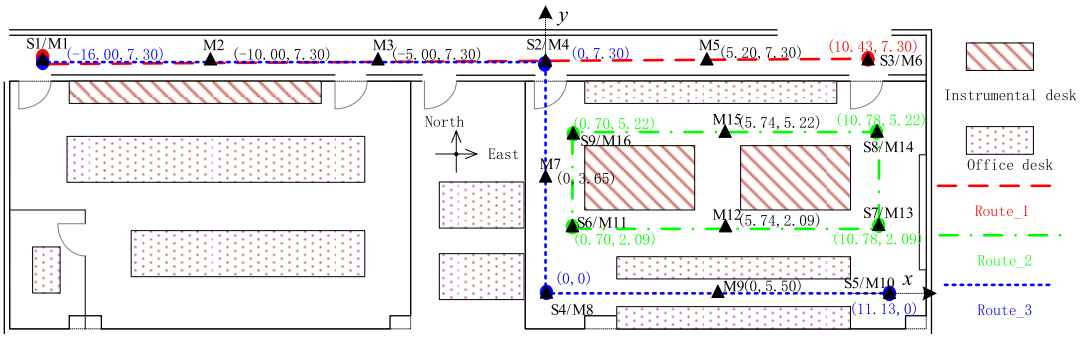

FIGURE 8. The routine and area layout of experiment.

TABLE 1. The parameter of IMU.

Parameter	Value
Sampling frequency	400Hz
Acceleration	3-axis, ± 16g
Gyroscope	3-axis, ± 2000dps
Resolution ratio	0.01°

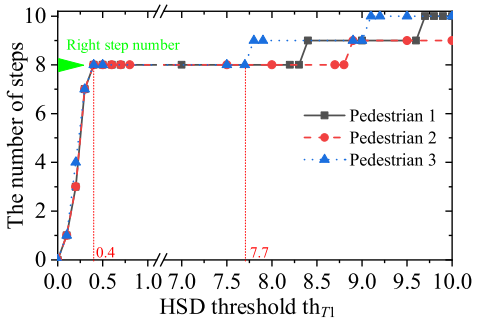

FIGURE 9. The relationship between number of steps and HSD threshold thT1.

origin of the coordinate. The black triangle markers are reference points used for performance evaluation. Three walking experiments are conducted in room (Routine_2), corridor (Routine_1), hybrid scene (Routine_1), respectively. Due to the sensor being fixed on the shoe, the height of sensor can be considered as zero when a valid step is detected, thus only 2D coordinates are calculated in later position estimation. It should be emphasized that the UWB anchor positions do not been marked in Fig. 8, and the anchor positions are listed in Table 2.

In order to achieve better localization result, the KF related parameters should be set properly. In our proposed system, the covariance matrix process noise, $\boldsymbol{Q}_{\mathrm{k}}$, is initialized as $\boldsymbol{Q}_1 = \mathrm{diag}([1 \times 10^4_{1\times3}, 1 \times 10^{-4}_{1\times3}, \boldsymbol{0}_{1\times3}])$, the initial measurement noise covariance matrix, $\boldsymbol{R}_{\mathrm{k}}$, is set as $\boldsymbol{R}_1 = \mathrm{diag}([\boldsymbol{0}_{1\times3}, 1 \times 10^{-2}_{1\times1}])$, and the state estimation covariance matrix, $\boldsymbol{P}_{\mathrm{k|k-1}}$, are initialized as $\boldsymbol{P}_0 = \mathrm{diag}([\boldsymbol{0}_{1\times3}, 1 \times 10^{-2}_{1\times3}, 1 \times 10^{-2}_{1\times3}])$, where the function diag(·) is a diagonal matrix.

The threshold th_{T1} of T1 in HSD can affect tracking performance directly, if th_{T1} is too large or small, it will result in wrong number of steps and invalid zero-velocity intervals. In order to depict the relationship between HSD threshold th_{T1} and the detected step number (number of zero-velocity

TABLE 2. The anchor position in experiment.

Test_1		Test_2		Test_3	
PDR	DSCLS	PDR	DSCLS	PDR	DSCLS
-	(-1.2, 8)	-	(3.1, 0.8)	-	(-13, 8) (5.6, 4.5)[1]

[1]Though there are two anchors used in Test_3, only one measure is selected for position estimation

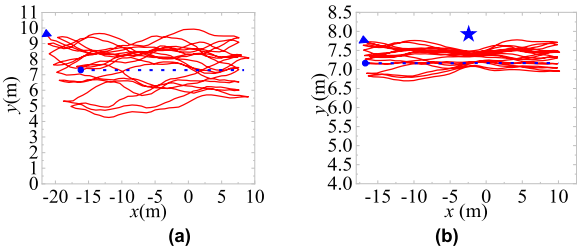

FIGURE 10. Test_1 results.

intervals). Three tests are carried out by three different pedestrians, and all of pedestrians are told to walk eight steps randomly. After that, we change the threshold th_{T1} of HSD (with an accuracy of 0.1) to detect the number of steps and give the corresponding graph in Fig. 9. As is shown in Fig. 9, the step number are correctly detected in all tests when the threshold th_{T1} is between 0.4 and 7.7. Thus, the threshold th_{T1} is set as 1 in this work.

As shown in Fig. 8, three test experiments (Test_1, Test_2, Test_3) are carried out along three different routines (Routine_1, Routine_2, Routine_3), respectively. Routine_1 walking sequence is S1-S2-S3-S2-S1 (52.86m). Routine_2 walking sequence is defined as S6-S7-S8-S9-S6 (26.42m). Routine_3 walking sequence is S1-S2-S4-S5-S4-S2-S1 (68.86m). In the Test_1, a subject repeats Routine_1 for 10 times with 683 steps, the total distance is 528.60m and the duration of Test_1 is 452.4s. In Test_2, the Routine_2 has been repeated 25 times with 660.5m distance, the number of step and the duration of Test_2 are 1042 and 539.3s, respectively. The duration of Test_3 is 687.6s after repeating Routine_3 12 times, it produces 1186 steps and 826.32m distance. The anchor positions in different tests are listed in Table 2.

V. RESULTS AND DISCUSSIONS

The traces of three tracking experiments (Test_1, Test_2, Test_3) estimated by PDR and our proposed DSCLS are

TABLE 3. Experiment result statistics between PDR and DSCLS.

		Total Distance (m)/Percentage	Average Position Error (m)	Last Position / Estimation Error (m)	Step Detection/ Percentage
Test_1	PDR	569.65/107.77%	3.27	(-21.39, 9.62)/5.98	707/103.51%
	Proposed	532.85/100.80%	0.56	(-17.07, 7.76)/1.17	677/99.12%
Test_2	PDR	790.22/119.64%	3.06	(3.79, -4.13)/6.94	1097/105.31%
	Proposed	670.54/101.52%	0.49	(0.98, 1.52)/0.63	1037/99.56%
Test_3	PDR	1146.18 /138.71%	4.43	(-30.45, 2.53)/15.22	1264/106.58%
	Proposed	848.88/102.73%	0.47	(-16.77, 7.05)/0.81	1179/99.40%

TABLE 4. Experiment result statistics between different people.

		Target 1	Target 2	Target 3	Target 4	Target 5
Average Step length (m)		0.63	0.51	0.45	0.56	0.71
Average Position Error (m)/	Proposed	0.49/84.49%	0.56/83.95%	0.61/83.78%	0.64/84.04%	0.76/84.10%
Error Reduced Percentage	PDR	3.16	3.49	3.76	4.01	4.78
Step Detection/Percentage		1042	1295	1468	1179	930
Last Position Error (m)		0.63	0.42	0.65	0.43	0.57

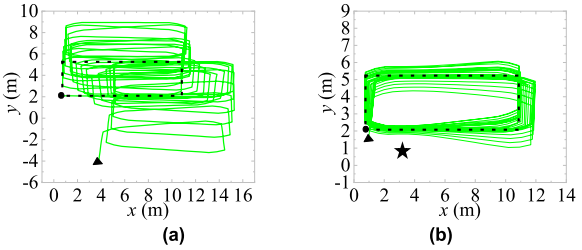

FIGURE 11. Test_2 results.

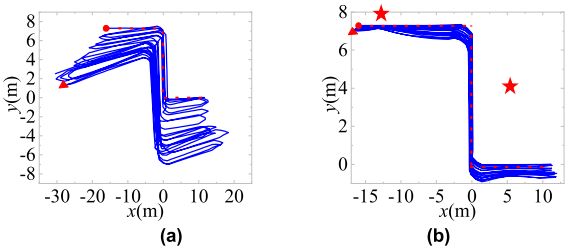

FIGURE 12. Test_3 results.

illustrated in Fig. 10, Fig. 11 and Fig. 12, respectively. It shows that sub-figure (a) is the tracking result estimated by PDR, whereas sub-figure (b) denotes the tracking result estimated by the proposed DSCLS. In sub-figure (b), the marker five-pointed stars are the position of UWB anchors. In each figure, the dash line is the reference route, and the estimated trace starts and ends at a dot and a triangle, respectively.

In this work, the reference routes start and end at same location, thus the marks in the first and the last estimated position can indicate the accuracy of the localization system. The errors in step detection, step length and direction estimation will result in distance estimation error and the trace shift. The tracking results provided by PDR shown in sub-figure (a) indicate that there exist severe errors in step detection, step length and orientation estimation. More specifically, the drift and bias in gyroscope of IMU sensor tilt the estimated trace, and step length and step detection errors will incur distance error in PDR. It is observed in sub-figure (b) that, compared with PDR in sub-figure (a), the general traces estimated by DSCLS has higher accuracy. Due to direction correcting function of DSCLS detailed in ***the heading angle and step length optimization*** section, the closer distance between pedestrian and UWB anchor is, the higher estimation accuracy will get. Therefore, it can be seen from the sub-figure (b) that the trace around anchor matches reference track more closely. Moreover, the last positions shown in sub-figure (b) are closer to the actual points. It should be emphasized that, in Fig. 12 (b), only one anchor with better communication condition is selected to estimation pedestrian position during space changing between corridor and room.

The corresponding tracking performance statistics are listed in Table 3. As presented in the table, compared with PDR, the total distances estimated by DSCLS are much closer to true values. The average position errors are calculated by using reference points on the given routes. In test_1, the average position and last position error of DSCLS is 0.56m and 1.17m, respectively. Compared with PDR average position error 3.27m and last position error 5.98m, the UWB assisted DSCLS reduces corresponding errors by 82.87% and 80.43%, respectively. In Test_2, using the proposed DSCLS, compared with PDR, the average position error is reduced by 83.99%, and the corresponding last position error decrement ratio is 90.92%. In Test_3, the average position error and last position error in DSCLS are reduced by 89.39% and 94.68%, respectively. There are two group of ranging measures for selecting in Test_3, hence, the accuracy improvement in Test_3 is larger compared with Test_1 and Test_2. In step detection part shown in Table 3, the percentage after slash is the ratio between estimated number and actual one. Compared with traditional step judging way, DSCLS has stricter step detection mechanism, thus, there may exit missed steps, and DSCLS has higher accuracy in step detection.

The Cumulative Distribution Function (CDF) of position error shown in Fig. 13 illustrates the error distribution in our

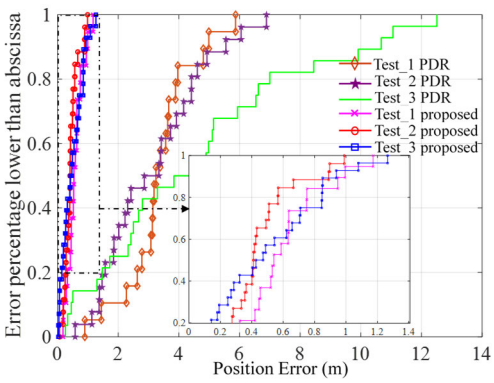

FIGURE 13. The Cumulative Distribution Function of position error.

TABLE 5. Performance comparison.

·	[24]	[28]	[36]	Proposed
Number of Anchors	5	1	3	1
Total Distance (m)	~30	276.0/436.8	~50	528.6/ 660.5/826.3
Average Position Error (m)	0.30	0.60/0.58	0.5	0.47/0.49/0.56
Step Length Correcting	NO	NO	NO	YES
Heading Correcting	YES	YES	YES	YES

proposed system. It shows that 85% position errors in proposed DSCLS are below 1m which verifies the effectiveness of the system.

In order to verify the stability of the proposed system, four more targets (target 2-5) have repeated Test_2, the corresponding experiment results are listed in Table 4. It shows that the percentage of average error reduction provided by the proposed system stabilizes at around 84% under different target tests, which proves the stability of system. It also can be seen that the largest fluctuation of average position error between different targets is reduced from 1.62m to 0.27m, which verifies the validity of proposed DSCLS.

The performance of proposed DSCLS is compared with existing fusion localization works in recent years, as listed in Table 5. One UWB anchor assisted PDR localization system is designed in [28], though this work improves the position accuracy greatly, its tracking device must be keeping in front of pedestrian and staying stable, this may limit its application range compared with our proposed foot mounted sensor; The algorithms proposed in [24] and [36] achieve higher localization accuracy, while these solutions are designed with multiple UWB anchors and verified with short distance tests. In this paper, the total testing distance is more than 2000m, and the step length correcting and direction constrained system are embedded in positioning frame which can provide more stable results.

VI. CONCLUSION

A Direction and Step Correction Localization System (DSCLS) is proposed in this paper. It consists of commercial INS sensor and one anchor UWB system which highly reduces the deployment time and cost. In order to achieve high-accuracy step detection and proper zero-velocity interval selection in INS, a modified step detection and zero-velocity selection approach called Heuristic Step Detection (HSD) is designed and used in DSCLS by evaluating readings of gyroscope and acceleration in IMU sensor. Afterwards, a pre-correction process is used to calibrate heading direction using UWB ranging measures and HSD through Kalman-type filer followed by a constrained sigma point based filter. And then, according to UWB ranging results, the step length and pedestrian direction are recorrected, it relates the heading direction to the step length and provides more stable location estimation results. The corresponding tracking experiments are conducted in three scenarios, and it verifies that the proposed system has long-term stable positioning performance with high step detection accuracy and strong error correction capability.

Our future works will focus on reducing the complexity of this algorithm. Moreover, the high-density UWB label with one UWB anchor fusion strategy should be also considered in practical application environment.

REFERENCES

[1] G. Li, Q. Sun, L. Boukhatem, J. Wu, and J. Yang, "Intelligent vehicle-to-vehicle charging navigation for mobile electric vehicles via VANET-based communication," *IEEE Access*, vol. 7, pp. 170888–170906, 2019.
[2] L. A. M. Hernández, S. P. Arteaga, G. S. Pérez, A. L. S. Orozco, and L. J. G. Villalba, "Outdoor location of mobile devices using trilateration algorithms for emergency services," *IEEE Access*, vol. 7, pp. 52052–52059, 2019.
[3] F. Yu and S. Jiang, "Mining location influence for location promotion in location-based social networks," *IEEE Access*, vol. 6, pp. 73444–73456, 2018.
[4] J. Li, H. Shi, H. Li, and A. Zhang, "Quad-band probe-fed stacked annular patch antenna for GNSS applications," *IEEE Antennas Wireless Propag. Lett.*, vol. 13, pp. 372–375, 2014.
[5] B. Li, Z. Hao, and X. Dang, "An indoor location algorithm based on Kalman filter fusion of ultra-wide band and inertial measurement unit," *AIP Adv.*, vol. 9, no. 8, Aug. 2019, Art. no. 085210, doi: 10.1063/1.5117341.
[6] Q. Tian, Z. Salcic, K. I.-K. Wang, and Y. Pan, "A multi-mode dead reckoning system for pedestrian tracking using smartphones," *IEEE Sensors J.*, vol. 16, no. 7, pp. 2079–2093, Apr. 2016, doi: 10.1109/JSEN.2015.2510364.
[7] X. Tao, X. Zhang, F. Zhu, F. Wang, and W. Teng, "Precise displacement estimation from time-differenced carrier phase to improve PDR performance," *IEEE Sensors J.*, vol. 18, no. 20, pp. 8238–8246, Oct. 2018, doi: 10.1109/JSEN.2018.2867225.
[8] A. R. Jimenez, F. Seco, J. C. Prieto, and J. Guevara, "Indoor pedestrian navigation using an INS/EKF framework for yaw drift reduction and a foot-mounted IMU," in *Proc. 7th Workshop Positioning, Navigat. Commun.*, Dresden, Germany, Mar. 2010, pp. 135–143, doi: 10.1109/WPNC.2010.5649300.
[9] H. Zhao, Z. Wang, S. Qiu, Y. Shen, L. Zhang, K. Tang, and G. Fortino, "Heading drift reduction for foot-mounted inertial navigation system via multi-sensor fusion and dual-gait analysis," *IEEE Sensors J.*, vol. 19, no. 19, pp. 8514–8521, Oct. 2019, doi: 10.1109/JSEN.2018.2866802.
[10] W. You, F. Li, L. Liao, and M. Huang, "Data fusion of UWB and IMU based on unscented Kalman filter for indoor localization of quadrotor UAV," *IEEE Access*, vol. 8, pp. 64971–64981, 2020, doi: 10.1109/ACCESS.2020.2985053.
[11] M. Narasimhappa, A. D. Mahindrakar, V. C. Guizilini, M. H. Terra, and S. L. Sabat, "MEMS-based IMU drift minimization: Sage husa adaptive robust Kalman filtering," *IEEE Sensors J.*, vol. 20, no. 1, pp. 250–260, Jan. 2020, doi: 10.1109/JSEN.2019.2941273.
[12] Y. Alvarez and F. L. Heras, "ZigBee-based sensor network for indoor location and tracking applications," *IEEE Latin Amer. Trans.*, vol. 14, no. 7, pp. 3208–3214, Jul. 2016, doi: 10.1109/TLA.2016.7587622.

[13] V. Bianchi, P. Ciampolini, and I. De Munari, "RSSI-based indoor localization and identification for ZigBee wireless sensor networks in smart homes," *IEEE Trans. Instrum. Meas.*, vol. 68, no. 2, pp. 566–575, Feb. 2019, doi: 10.1109/TIM.2018.2851675.
[14] S. Pack, G. Park, and H. Ko, "An SIP-based location management framework in opportunistic WiFi networks," *IEEE Trans. Veh. Technol.*, vol. 64, no. 11, pp. 5269–5274, Nov. 2015, doi: 10.1109/TVT.2014.2377047.
[15] S. Li, M. Hedley, K. Bengston, D. Humphrey, M. Johnson, and W. Ni, "Passive localization of standard WiFi devices," *IEEE Syst. J.*, vol. 13, no. 4, pp. 3929–3932, Dec. 2019, doi: 10.1109/JSYST.2019.2903278.
[16] A. R. J. Ruiz and F. S. Granja, "Comparing ubisense, BeSpoon, and DecaWave UWB location systems: Indoor performance analysis," *IEEE Trans. Instrum. Meas.*, vol. 66, no. 8, pp. 2106–2117, Aug. 2017, doi: 10.1109/TIM.2017.2681398.
[17] M.-G. Li, H. Zhu, S.-Z. You, and C.-Q. Tang, "UWB-based localization system aided with inertial sensor for underground coal mine applications," *IEEE Sensors J.*, vol. 20, no. 12, pp. 6652–6669, Jun. 2020, doi: 10.1109/JSEN.2020.2976097.
[18] C. Perera, S. Aghaee, R. Faragher, R. Harle, and A. F. Blackwell, "Contextual location in the home using Bluetooth beacons," *IEEE Syst. J.*, vol. 13, no. 3, pp. 2720–2723, Sep. 2019, doi: 10.1109/JSYST.2018.2878837.
[19] J. Lovon-Melgarejo, M. Castillo-Cara, O. Huarcaya-Canal, L. Orozco-Barbosa, and I. Garcia-Varea, "Comparative study of supervised learning and Metaheuristic algorithms for the development of bluetooth-based indoor localization mechanisms," *IEEE Access*, vol. 7, pp. 26123–26135, 2019, doi: 10.1109/ACCESS.2019.2899736.
[20] A. Booranawong, N. Jindapetch, and H. Saito, "Adaptive filtering methods for RSSI signals in a device-free human detection and tracking system," *IEEE Syst. J.*, vol. 13, no. 3, pp. 2998–3009, Sep. 2019, doi: 10.1109/JSYST.2019.2919642.
[21] J. P. Beaudeau, M. F. Bugallo, and P. M. Djuric, "RSSI-based multi-target tracking by cooperative agents using fusion of cross-target information," *IEEE Trans. Signal Process.*, vol. 63, no. 19, pp. 5033–5044, Oct. 2015, doi: 10.1109/TSP.2015.2448530.
[22] K. Yu, K. Wen, Y. Li, S. Zhang, and K. Zhang, "A novel NLOS mitigation algorithm for UWB localization in harsh indoor environments," *IEEE Trans. Veh. Technol.*, vol. 68, no. 1, pp. 686–699, Jan. 2019, doi: 10.1109/TVT.2018.2883810.
[23] K. Zhang, C. Shen, Q. Zhou, H. Wang, Q. Gao, and Y. Chen, "A combined GPS UWB and MARG locationing algorithm for indoor and outdoor mixed scenario," *Cluster Comput.*, vol. 22, no. S3, pp. 5965–5974, May 2019.
[24] Y. Xu, C. K. Ahn, Y. S. Shmaliy, X. Chen, and Y. Li, "Adaptive robust INS/UWB-integrated human tracking using UFIR filter bank," *Measurement*, vol. 123, pp. 1–7, Jul. 2018.
[25] J. Zhu and S. S. Kia, "UWB ranging aided pedestrian geolocation with GPB-based filtering for LoS and NLoS measurement processing," in *Proc. IEEE/ION Position, Location Navigat. Symp. (PLANS)*, Portland, OR, USA, Apr. 2020, pp. 781–787, doi: 10.1109/PLANS46316.2020.9110175.
[26] J. Zhu and S. S. Kia, "Bias compensation for UWB ranging for pedestrian geolocation applications," *IEEE Sensors Lett.*, vol. 3, no. 9, pp. 1–4, Sep. 2019, doi: 10.1109/LSENS.2019.2936007.
[27] Q. Fan, B. Sun, Y. Sun, and X. Zhuang, "Performance enhancement of MEMS-based INS/UWB integration for indoor navigation applications," *IEEE Sensors J.*, vol. 17, no. 10, pp. 3116–3130, May 2017, doi: 10.1109/JSEN.2017.2689802.
[28] Q. Tian, K. I.-K. Wang, and Z. Salcic, "A low-cost INS and UWB fusion pedestrian tracking system," *IEEE Sensors J.*, vol. 19, no. 10, pp. 3733–3740, May 2019, doi: 10.1109/JSEN.2019.2894714.
[29] Y. Li, Y. Zhuang, H. Lan, Q. Zhou, X. Niu, and N. El-Sheimy, "A hybrid WiFi/magnetic matching/PDR approach for indoor navigation with smartphone sensors," *IEEE Commun. Lett.*, vol. 20, no. 1, pp. 169–172, Jan. 2016.
[30] Q. Xu, X. Li, and C.-Y. Chan, "Enhancing localization accuracy of MEMS-INS/GPS/In-vehicle sensors integration during GPS outages," *IEEE Trans. Instrum. Meas.*, vol. 67, no. 8, pp. 1966–1978, Aug. 2018, doi: 10.1109/TIM.2018.2805231.
[31] A. R. J. Ruiz, F. S. Granja, J. C. P. Honorato, and J. I. G. Rosas, "Accurate pedestrian indoor navigation by tightly coupling foot-mounted IMU and RFID measurements," *IEEE Trans. Instrum. Meas.*, vol. 61, no. 1, pp. 178–189, Jan. 2012.
[32] J. B. Kristensen, M. M. Ginard, O. K. Jensen, and M. Shen, "Non-line-of-sight identification for UWB indoor positioning systems using support vector machines," in *IEEE MTT-S Int. Microw. Symp. Dig.*, Guangzhou, China, May 2019, pp. 1–3, doi: 10.1109/IEEE-IWS.2019.8804072.
[33] Q. Tian, K. I.-K. Wang, and Z. Salcic, "An INS and UWB fusion approach with adaptive ranging error mitigation for pedestrian tracking," *IEEE Sensors J.*, vol. 20, no. 8, pp. 4372–4381, Apr. 2020, doi: 10.1109/JSEN.2020.2964287.
[34] L. Zheng, W. Zhou, W. Tang, X. Zheng, A. Peng, and H. Zheng, "A 3D indoor positioning system based on low-cost MEMS sensors," *Simul. Model. Pract. Theory*, vol. 65, pp. 45–56, Jun. 2016.
[35] E. Allseits, V. Agrawal, J. Lučarević, R. Gailey, I. Gaunaurd, and C. Bennett, "A practical step length algorithm using lower limb angular velocities," *J. Biomech.*, vol. 66, pp. 137–144, Jan. 2018.
[36] Y. Xu, C. K. Ahn, Y. S. Shmaliy, X. Chen, and L. Bu, "Indoor INS UWB-based human localization with missing data utilizing predictive UFIR filtering," *IEEE/CAA J. Automatica Sinica*, vol. 6, no. 4, pp. 952–960, Jul. 2019, doi: 10.1109/JAS.2019.1911570.

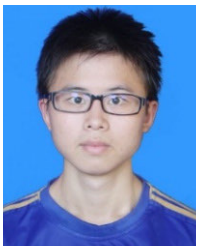

KELIU LONG (Graduate Student Member, IEEE) was born in 1993. He received the M.S. degree in communication and information system from the Jiangxi University of Science and Technology, Jiangxi, China. He is currently pursuing the Ph.D. degree in information and communication engineering with Hainan University, Hainan, China. His current research interests include memristor neural networks, indoor inertial navigation, and localization.

CHONG SHEN (Member, IEEE) was born in 1981. He received the Ph.D. degree from the Cork Institute of Technology, Ireland, in 2008. From 2008 to 2009, he was a full-time Postdoctoral Research Fellow with the Tyndall National Institute, Ireland. He is currently a Professor with the College of Information Science Technology, Hainan University. He is the author of over 100 articles published in related journals and international conference proceedings. His major research interests include ultra-wideband communications, wireless communications, sensor networks, the Internet of Things, and embedded systems research. He has served as a Reviewer of over ten journals.

CHUAN TIAN is currently a Professor with the Institute of Deep-sea Science and Engineering, Chinese Academy of Sciences (IDSSE, CAS). He is also the Vice Director of the Deep Sea Engineering Technology Department. He is also a Ph.D. Supervisor with the University of Chinese Academy of Sciences (UCAS). He leads more than ten projects in the National Natural Science Foundation of China (General Program) and the National Key Reach and Development Program of China. He has Strategic pioneering science and technology Program of Chinese Academy of Sciences. He has published more than 20 SCI/EI papers and 11 granted patents. His major research interests include technology of deep-sea sensor and real-time deep sea observation platform integration.

KUN ZHANG (Member, IEEE) was born in 1981. He is currently pursuing the Ph.D. degree with the College of Information Science and Technology, Hainan University, Haikou, China. He is also a Professor with Hainan Tropical Ocean University. He is the author of over 100 articles published in related journals. His major research interests include intelligent data analysis and data mining, ultra-wideband communications, wireless communications, sensor networks, the Internet of Things, and embedded systems.

UZAIR ASLAM BHATTI was born in 1986. He received the Ph.D. degree, in June 2019. He is currently pursuing the Ph.D. degree in implementing Clifford algebra algorithms in analyzing the geo spatial data using AI with Nanjing Normal University. His research interests include artificial intelligence, machine learning, and image processing.

DARRYL FRANCK NSALO KONG was born in Douala, Cameroon, in 1991. He received the master's degree in software engineering from Zhejiang Normal University, in 2017. He is currently pursuing the Ph.D. degree with Hainan University. His research interests include marine communication, the Internet of Things, and sensor networks.

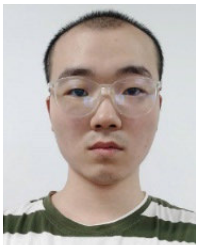

SHUO FENG graduated from Dalian Maritime University. He is currently pursuing the degree with the State Key Laboratory of Marine Resources Utilization in South China Sea, Hainan University. He is major in electronic and communication engineering. His research interests include indoor UWB positioning and machine learning.

HESEN CHENG graduated from Xidian University. He is currently pursuing the degree with the State Key Laboratory of Marine Resources Utilization in South China Sea, Hainan University. His research interests include image processing and indoor UWB positioning.